

Voltage-tunable, femtometer-precision plasmo-mechanical displacement at fixed gap size

Rasim Volga Ovali¹ and Mehmet Emre Tasgin²

¹*Recep Tayyip Erdogan University, 53100 Rize, Turkey*

²*Institute of Nuclear Sciences, Hacettepe University, 06800 Ankara, Turkey*

(Dated: May 8, 2025)

We propose an elegant method for continuous electrical-tuning of plasmo-mechanical displacement and squeezing without changing plasmonic gap size. Recent experiments bend the mechanical oscillator (cantilever) in units of nm via electrostatic actuators. We do not bend the cantilever but merely electrically-tune the gap intensity, so plasmo-mechanical coupling, via Fano resonance. This allows continuous displacement tuning in units of mechanical oscillator length that is about 30 fm in the experiments. This way, coupling strength can be tuned by 2 orders-of-magnitude via only a 1 V potential difference. Response time is *picoseconds*. Moreover, quadrature-squeezing (entanglement) of the oscillator can also be tuned continuously.

I. INTRODUCTION

Coupling of a mechanical oscillator with light (optomechanics) possesses important implementations such as optical cooling of the mechanical motion [1], transfer of optical quantum states into mechanical ones [2], and for introducing light-controlled quantum superposition states [3] in the mechanical motion which made, for instance, detection of gravitational waves (LIGO) possible [4].

Plasmo-mechanics, a newly developing field, has the potential to carry these phenomena into smaller dimensions [5–13]. This field provides both controllability and integrability that are necessary for implementations with quantum circuits. Localized surface plasmons (LSPs), appearing at nm-sized metallic gaps, take the place of photons. LSPs confine light into hotspots (gap) where intensity can be enhanced by several orders of magnitude [6, 10, 11]. In plasmomechanics, the near-field excitations (plasmons) create the radiation pressure in analogy to photons. Plasmon-mechanical interaction becomes greatly enhanced compared to the conventional optomechanics.

Plasmonics can also provide control over the plasmo/opto-mechanical interactions. For instance, recent state-of-the-art experimental works demonstrate the electrical control of the plasmonic gap size, so the LSP resonances and the gap intensity [10, 11]. The LSP resonance appears in the gap between a cantilever, into which a cuboid gold nanostructure is embedded, and a gold pad lying at the bottom. See Fig. 1. Voltage applied on electrostatic actuator bends the equilibrium position of the cantilever, so the gap size changes between 20 nm–70 nm. This way, effective plasmomechanical coupling can be tuned substantially within a time of 10 nanoseconds. However, bending of the cantilever avoids the electrical-tuning of the displacement in the order of cantilever's oscillator strength, $x_{\text{ZPF}} \approx 30$ fm in Ref. [10], but allows a nm-size tuning only.

In this paper, we show that electrical tuning of gap plasmon intensity (so the effective plasmomechanical

coupling [14, 15]) can be achieved without bending the cantilever. The cantilever displacement is solely controlled by the radiation pressure of the gap intensity. This makes tuning of the displacement in units of $x_{\text{ZPF}} \approx 30$ fm possible. Response time is *picoseconds*. We utilize a Fano resonance (transparency) [16–20] induced by a layer of defect-centers (relies in the LSP gap) to turn off the gap intensity. See Fig. 1. We demonstrate the phenomenon via FDTD simulations using Lumerical. Application of only a 0.8 V potential difference is sufficient to continuously tune the gap intensity between 1–200. See Fig. 4. Our scheme is also compatible with sideband cooling [1] [21]. Not only the displacement but also quadrature-squeezing (can also be converted into entanglement [22, 23]) of the cantilever oscillations is tuned continuously. See Fig. 5. We use the experimental parameters [10] in our calculations.

The plasmomechanical system (Fig. 1) is excited by a laser of frequency ω ($\lambda = c/\omega$). A transparency takes place at the gap intensity (LSP) due to the Fano resonance (FR) [16–20]. Please compare Figs. 2 and 3. FR is induced by a densely-implanted defect-centers [24–26] layer (quantum emitter, QE). Such a transparency, which avoids also the optomechanical coupling, takes place when ω is around the level-spacing of the defect-centers Ω_{QE} , i.e., for $\omega = \omega_f \sim \Omega_{\text{QE}}$ [27]. The voltage applied on the defect-centers shifts the level-spacing Ω_{QE} with respect to the excitation frequency ω . Thus, the number of plasmons in the gap (Fig. 4), so the optomechanical coupling and the displacement (Fig. 5a), are continuously tuned.

FR is the plasmon analog of electromagnetically-induced transparency (EIT) formerly studied on atomic vapors [31]. Metal nanostructures (MNSs) localize the incident light on nm-sized hotspots (gaps) as plasmonic oscillations. When a QE is placed at one of the hotspots, a strong plasmon-QE coupling takes place. This introduces a narrow transparency window in the plasmon spectrum [16–19, 32]. A FR takes place in a narrow frequency band which makes it unuseful for broadband applications [33]. Such a disadvantage, however, turns

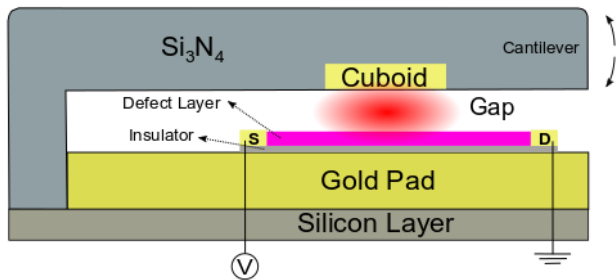


FIG. 1. Fano-control of plasmomechanical system. A gold cuboid of dimensions $20 \times 20 \times 40$ nm is embedded into the bottom side of a Si_3N_4 cantilever vibrating at frequency $\omega_m = 10$ MHz [6, 10]. A gap plasmon resonance occurs between the cuboid and the gold pad lying 20 nm below the cantilever. Incident light of frequency ω is along the z -direction. A layer of densely-implanted defect-centers [24–26] of resonance Ω_{QE} is placed on the pad. It creates a Fano transparency in the gap intensity at about the defect-resonance, i.e., $\omega = \omega_f \sim \Omega_{\text{QE}}$ [27]. The potential difference applied on the layer electrically-tunes the defect resonance [28–30], so also continuously tunes the gap intensity. The cantilever is not bended in difference to Refs. [10, 11].

out to be highly beneficial for electrical tuning of linear/nonlinear optical processes [34, 35] which is not available by other methods.

In our study, we utilize this transparency to turn off the gap plasmon occupation. As effective plasmomechanical coupling is suppressed, the noise-squeezing of the mechanical oscillator is also turned off. When the excitation frequency ω matches the transparency window, i.e., $\omega = \omega_f \sim \Omega_{\text{QE}}$ [27], the gap intensity turns off. Thus, plasmomechanical interaction is closed and no mechanical displacement appears. However, when Ω_{QE} is slightly shifted via an applied voltage [28–30], mechanical displacement (Fig. 4) and squeezing (Fig. 5) can be tuned continuously at a desired value.

It is worth nothing that experiments clearly demonstrate that plasmonic structures can handle quantum features, such as entanglement and noise-squeezing, much longer times compared to their typical damping times [36–41]. The latter damping is defined for flowing out of the field from the MNS while former governs the degrading of the quantum noise. In other words, degrading time for the squeezed-noise (solely determines the quantum optics features [42]) are much longer.

The paper is organized as follows. In Sec. II, we briefly mention about Fano resonances: how and why they appear in plasmonic spectra. In Sec. III, we present our finite difference time domain (FDTD) simulations. We show that the ordinarily very strong gap plasmon field is suppressed at $\omega = \omega_f \sim \Omega_{\text{QE}}$ by the presence of a defect-center layer. The intensity at the gap can be continuously tuned by slightly changing Ω_{QE} . In Sec. IV, we study the hamiltonian governing the plasmomechanical

interaction in the presence of the Fano resonance. We calculate the noise-squeezing in the mechanical motion using Langevin equations for the noise operators, e.g., $\delta\hat{a}$ [14, 15]. We show that the noise-squeezing can also be tuned continuously.

II. FANO RESONANCES

Coupling of a quantum object (QE) to a plasmon excitation introduces two paths for the absorption of the incident field. The two paths destructively interfere with each other and the absorption of incident field is canceled [32, 43]. Thus, a transparency in the plasmonic spectrum appears. This phenomenon can be demonstrated on a single equation [19]

$$\alpha_p = \frac{\varepsilon_p}{[i(\Omega_p - \omega) + \gamma_p] - \frac{y|f|^2}{i(\Omega_{\text{QE}} - \omega) + \gamma_{\text{QE}}}}. \quad (1)$$

Here, α_p is the plasmon amplitude. The plasmon mode, of resonance Ω_p ($\lambda_p = c/\Omega_p$) and damping rate γ_p , is pumped by an incident field of frequency ω and amplitude ε_p . The QE has a level-spacing of Ω_{QE} and a decay rate γ_{QE} . The coupling between the QE and the plasmon excitation, f , is highly enhanced due to the field localization at the hotspot. y is the population inversion. $\gamma_{\text{QE}} \simeq 10^{10}$ Hz is 4 orders of smaller than the plasmonic one $\gamma_p \sim 10^{14}$ Hz. ω and Ω_p are at optical frequencies $\sim 10^{15}$ Hz. Thus, in frequencies scaled with optical ones, $\omega \sim 1$, $\Omega_p \sim 1$, $\Omega_{\text{QE}} \sim 1$, $\gamma_p \sim 0.1$, $\gamma_{\text{QE}} \sim 10^{-5}$ and $f \simeq 0.1$ [16, 17, 44].

When the incident field ω is in resonance with the QE, i.e., $\omega \simeq \Omega_{\text{QE}}$, the $\gamma_{\text{QE}} \sim 10^{-5}$ leaves alone in the second term of the denominator. It comes out as a factor of 10^5 that multiplies the $y|f|^2$ term. Thus, the second term of the denominator becomes exceeding large compared to the first term. This suppresses the plasmon excitation amplitude α which creates a transparency at $\omega = \Omega_{\text{QE}}$.

The transparency takes place in a very narrow band for small γ_{QE} . We propose to tune Ω_{QE} via an applied voltage [28–30] which changes the gap intensity substantially. The experiments shows that 20 meV tuning in Ω_{QE} can easily be achieved only with a 1 V of applied potential difference [28, 29].

We note that Eq. (1) is derived from an analytical model which cannot account the retardation effects. That is, Eq. (1) is obtained as if all interactions with the normally extended plasmon field takes place at a single point. Retardation effects shift the spectral position of the FR, ω_f , more with respect to Ω_{QE} as LSP gap size becomes larger. So in the next section, we present a realistic demonstration of the phenomenon for a spatially extended plasmon profile. In Sec. IV, we calculate the entanglement/squeezing in a plasmomechanical system controlled by a FR.

III. FDTD SIMULATIONS

In this section, we provide exact solutions of the 3D Maxwell equations for a sample plasmomechanical system, i.e., similar to the one experimentally studied in Ref. [10]. A cuboid gold nanoparticle of dimensions $20 \times 20 \times 40$ nm is embedded into the lower face of a cantilever made of silicon nitride. There lies a gold pad 20 nm below the cantilever (also the cuboid). The gap between the two gold surfaces—the cuboid and the gold pad— supports a gap localized surface plasmon (LSP) resonance (LSPR). The LSP is excited by a z-polarized light. The gap plasmons interact with the cantilever (mechanical system) that supports mechanical oscillations at about $\omega_m = 10$ MHz. Zero point fluctuations (ZPF) of such a cantilever is reported to be about $x_{\text{ZPF}} \simeq 30$ fm in Ref. [10]. Thus, control of the gap intensity (See Fig. 2b) should be expected to tune the mechanical displacement in units of 30 fm [45].

First, we study the spectrum of the LSPRs. We carry out FDTD simulations in Lumerical using experimental dielectric functions for the silicon nitride and gold. In Fig. 2a we observe that the system supports two LSPRs centered at 533 nm and $\lambda_p = 610$ nm. We, as an instance, choose to study at the resonance $\lambda_p = 610$ nm. In Fig. 2b, we plot the gap intensity profile, for instance, at $\lambda = 598$ nm. Here we present the intensity profile at $\lambda = 598$ nm (i.e., not at the peak) merely because Fano transparency appears at $\lambda_f = 598$ nm in Fig. 3a when we place the defect-center layer. We aim a comparison.

After determining the LSPRs and the gap intensity profile, we aim to provide a simple demonstration of the Fano resonance (transparency) in such a system. We place a 3-nm-thick layer of QE standing for the densely-implemented defect-centers [24–26]. The layer is positioned on the gold pad and simulated by a Lorentzian dielectric function [16–18] of resonance $\Omega_{\text{QE}} = 610$ nm, linewidth $\gamma_{\text{QE}} = 10^{11}$ Hz and oscillator strength $f_{\text{osc}} = 0.1$ [16, 17].

In Fig. 3a we plot the spectrum obtained from a point monitor positioned 1 nm below the cuboid. We choose an increased number of frequency points in order to see if there appears a narrow transparency window. We observe that a transparency window appears at about $\lambda_f = 598$ nm which is not at the $\Omega_{\text{QE}} = 610$ nm. This is something to be expected as Eq. (1) is valid when retardation effects are ignored. This negligence certainly does not hold for a large plasmonic gap of 20 nm width [27].

In Fig. 3b, we plot the gap intensity profile at $\lambda = \lambda_f = 598$ nm. One can observe that gap intensity, so the plasmomechanical coupling, is suppressed substantially compared to Fig. 2b.

Next, we slightly shift Ω_{QE} step by step assuming that a varying voltage is applied on the defect layer. In Fig. 4 we show that mean gap intensity can be tuned between $120I_0$ and $30.000I_0$. Thus, our FDTD simulations clearly demonstrate that gap intensity, so the effective plasmomechanical coupling and mechanical displacement (in units of $x_{\text{ZPF}} \simeq 30$ fm) [14, 15] can be continuously tuned

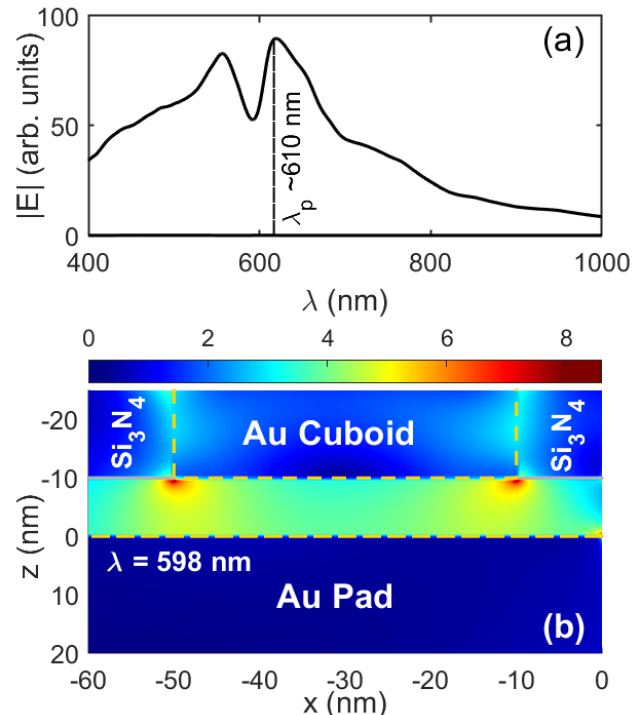


FIG. 2. (a) The plasmonic gap in Fig. 1 supports two LSP resonances at 533 nm and $\lambda_p = 610$ nm. (b) We plot the gap intensity for $\lambda = 598$ nm (i.e., not at the plasmonic peak) as we will compare it with the case when QE layer is present. In Fig. 3, Fano transparency appears at $\omega = \omega_f = 598$ nm.

by an applied voltage of only 0.8 V—the potential difference needed to tune Ω_{QE} from 2.035 eV to 2.042 eV [28–30] in Fig. 4.

IV. TUNING NOISE-SQUEEZING AND ENTANGLEMENT

Electrical tuning is also possible for quantum optical features of the Fano-controlled plasmomechanical system. Here, we show that displacement x_m , Fig. 5a, and the quadrature-squeezing of the mechanical motion, Fig. 5b, can also be continuously tuned via the applied voltage. The mechanical squeezing can either be used to reduce the uncertainty in the cantilever motion below the standard quantum limit, i.e., $x_{\text{ZPF}} \simeq 30$ fm in Ref. [10], or to generate entanglement between different oscillator(s) modes [22, 23].

Dynamics of the system can be summarized as follows. Incident light of frequency ω drives the gap LSPs. Incident field (intensity I_0) is localized at the hotspot where the local plasmon intensity becomes $\sim 10^4 \times I_0$ times the incident one. See Fig. 2a. The defect-center layer is placed into the gap. It lies on the gold pad. Thus, QE interacts with the plasmon mode strongly. Its interac-

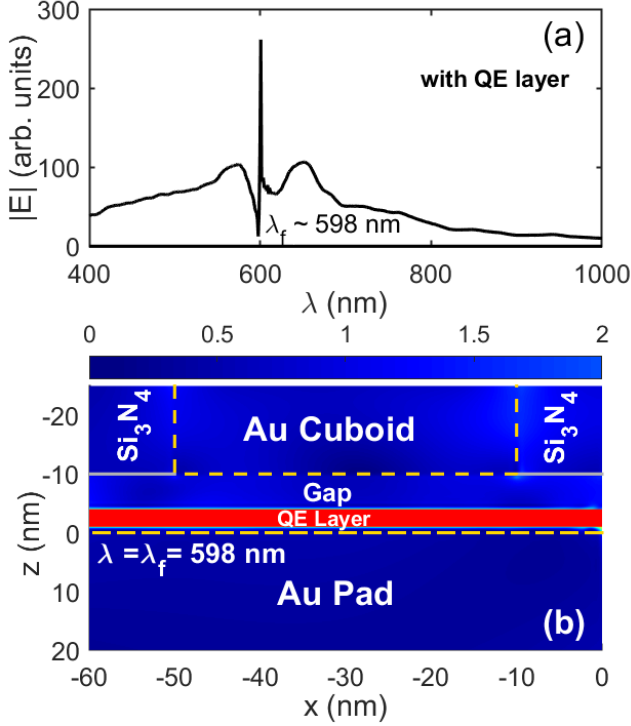


FIG. 3. (a) The defect layer of resonance $\Omega_{QE} = 610$ nm introduces a Fano resonance (transparency) at $\omega = \omega_f = 598$ nm. The shift from Ω_{QE} is due to retardation effect [27]. (b) The FR turns off the gap intensity so the effective plasmomechanical coupling. Thus, by changing the defect resonance Ω_{QE} , via an applied voltage, one can tune the gap intensity at a fixed driving frequency, e.g., 598 nm. See Fig. 4. The peak at 602 nm is Fano enhancement effect [19, 44].

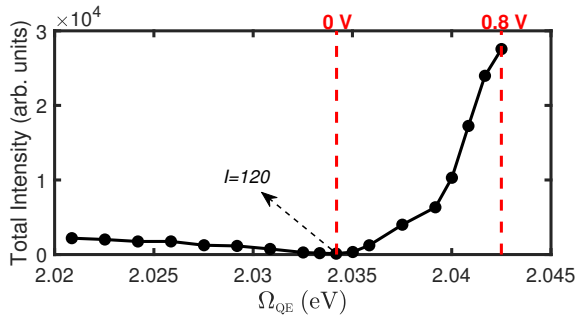


FIG. 4. Continuous electrical-tuning of the gap intensity by shifting the Fano resonance via applied voltage [28, 29]. One volt potential difference is more than enough to tune the gap intensity between $120I_0 - 30.000I_0$ (or 200 times). Plasmomechanical coupling, cantilever displacement and entanglement is tuned in the same manner [14, 15].

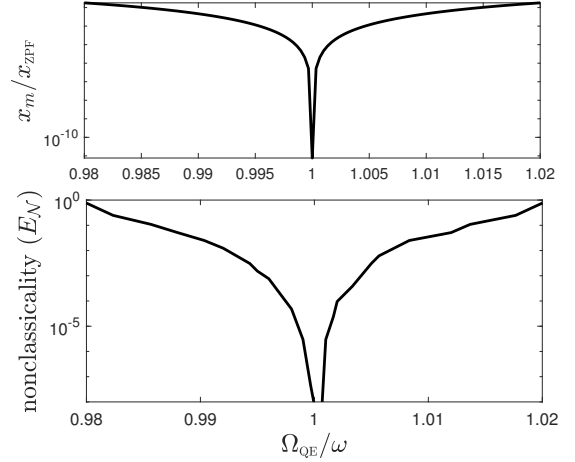


FIG. 5. (a) Displacement and (b) quantumness of the oscillator motion can also be electrically tuned in a continuous manner. Quantumness (e.g. squeezing) of the mechanical motion is quantified in terms of log-neg [48, 49], entanglement such a single-mode generates when it is divided into two at a beam-splitter [47, 50]. Displacement is scaled with $x_{ZPF} = 30$ fm given in Ref. [10].

tion with the incident field becomes very weak compared to the plasmons. (Note the 4 orders-of-magnitude ratio between the two intensities.) The gap plasmon intensity also applies a radiation pressure that induces a coupling between the mechanical vibrations $\hat{x}_m = (\hat{a}_m^\dagger + \hat{a}_m)/\sqrt{2}$ and the plasmon mode \hat{a} .

Total hamiltonian can be written as

$$\hat{\mathcal{H}} = \hbar\omega_m \hat{a}_m^\dagger \hat{a}_m + \hbar\Omega \hat{a}^\dagger \hat{a} + \hbar\varepsilon_p (\hat{a}^\dagger e^{-i\omega t} + \hat{a} e^{i\omega t}) + \hbar\omega_{eg} |e\rangle\langle e| + \hbar g \hat{a}^\dagger \hat{a} \hat{x}_m + \hbar f (\hat{a}|e\rangle\langle g| + \hat{a}^\dagger |g\rangle\langle e|), \quad (2)$$

where the terms are, respectively, energy of the mechanical oscillations, plasmons, the coupling to the incident field, excitation energy of the QE, radiation pressure interaction and QE-plasmon coupling that induces the Fano transparency.

We calculate the entanglement features using the standard methods [14, 15] that can be found in the literature. See the supplementary material (SM) [46]. In Fig. 5a, we present the expectation value of the cantilever displacement in units of $x_{ZPF} \simeq 30$ fm given in Ref. [10]. Fig. 5b plots the nonclassicality (e.g., squeezing) in units of its entanglement potential [47]. This quantifies how much entanglement is generated when a single squeezed mode is splitted into two in a beam-splitter. The applied voltage tunes the gap intensity, so the effective coupling $G = \alpha_p \times g$ [14, 15]. Smaller G results in smaller displacement and entanglement. We use the parameters of Ref. [10].

V. SUMMARY AND OUTLOOKS

In summary, we provide a device where we can control the plasmomechanical coupling by a factor of 200. We do not tilt the cantilever equilibrium position. Instead, we gradually turn on and off the gap plasmon intensity via an applied voltage. This is not only faster (ps) than tuning the driving optical field intensity, but also provides enhanced integrability. (In order to appreciate, please consider a number of these devices integrated at different places to a circuit. One would need to tune each driving intensity separately that would necessitate much larger spaces. In our method, however, a common drive, i.e., a waveguide, space for light would be sufficient.)

We utilize the Fano transparency induced by a quantum object (layer of defect-centers) in order to tune the gap intensity. This way, we can achieve very high pre-

cision cantilever displacements (units of 30 fermimeters) without bending the cantilever that limits the precision with nm. Moreover, we can controllably tune (reduce) the noise in the mechanical displacement x_m . On top of this, the typical response time for such a tuning in our system is in picoseconds, thus limited only by the speed of the device tuning the applied voltage. Such a fast and precision controlled displacement cannot be achieved with other configuration to our best knowledge. Naturally, one needs sideband cooling [1] at room temperature or needs to work at cryogenic temperatures in order to achieve such precisions.

We should renote that such precise displacement tunings are already available in optomechanics at room temperature via sideband cooling technique [1]. However, one controls the pump intensity.

-
- [1] M Bhattacharya and P Meystre. Trapping and cooling a mirror to its quantum mechanical ground state. *Physical Review Letters*, 99(7):073601, 2007.
- [2] Jing Zhang, Kunchi Peng, and Samuel L Braunstein. Quantum-state transfer from light to macroscopic oscillators. *Physical Review A*, 68(1):013808, 2003.
- [3] Pierre Meystre. A short walk through quantum optomechanics. *Annalen der Physik*, 525(3):215–233, 2013.
- [4] Wenxuan Jia, Victoria Xu, Kevin Kuns, Masayuki Nakano, Lisa Barsotti, Matthew Evans, Nergis Mavalvala, LIGO Scientific Collaboration†, R Abbott, I Abouelfettouh, et al. Squeezing the quantum noise of a gravitational-wave detector below the standard quantum limit. *Science*, 385(6715):1318–1321, 2024.
- [5] Rutger Thijssen, Ewold Verhagen, Tobias J Kippenberg, and Albert Polman. Plasmon nanomechanical coupling for nanoscale transduction. *Nano Letters*, 13(7):3293–3297, 2013.
- [6] Brian J Roxworthy and Vladimir A Aksyuk. Nanomechanical motion transduction with a scalable localized gap plasmon architecture. *Nature Communications*, 7(1):13746, 2016.
- [7] Jun-Yu Ou, Eric Plum, Jianfa Zhang, and Nikolay I Zheludev. Giant nonlinearity of an optically reconfigurable plasmonic metamaterial. *Advanced Materials*, 28(4):729–733, 2016.
- [8] Hai Zhu, Fei Yi, and Ertugrul Cubukcu. Plasmonic metamaterial absorber for broadband manipulation of mechanical resonances. *Nature Photonics*, 10(11):709–714, 2016.
- [9] Biqin Dong, Xiangfan Chen, Fan Zhou, Chen Wang, Hao F Zhang, and Cheng Sun. Gigahertz all-optical modulation using reconfigurable nanophotonic metamolecules. *Nano letters*, 16(12):7690–7695, 2016.
- [10] Brian J Roxworthy and Vladimir A Aksyuk. Electrically tunable plasmomechanical oscillators for localized modulation, transduction, and amplification. *Optica*, 5(1):71–79, 2018.
- [11] Christian Haffner, Andreas Joerg, Michael Doderer, Felix Mayor, Daniel Chelladurai, Yuriy Fedoryshyn, Cosmin Ioan Roman, Mikael Mazur, Maurizio Burla, Henri J Lezec, et al. Nano-opto-electro-mechanical switches operated at cmos-level voltages. *Science*, 366(6467):860–864, 2019.
- [12] Nan Xu, Ze-Di Cheng, Jin-Dao Tang, Xiao-Min Lv, Tong Li, Meng-Lin Guo, You Wang, Hai-Zhi Song, Qiang Zhou, and Guang-Wei Deng. Recent advances in nano-opto-electro-mechanical systems. *Nanophotonics*, 10(9):2265–2281, 2021.
- [13] Alemayehu Nana Koya, Joao Cunha, Karina Andrea Guerrero-Becerra, Denis Garoli, Tao Wang, Saulius Juodkazis, and Remo Proietti Zaccaria. Plasmomechanical systems: principles and applications. *Advanced Functional Materials*, 31(41):2103706, 2021.
- [14] Claudiu Genes, Andrea Mari, Paolo Tombesi, and David Vitali. Robust entanglement of a micromechanical resonator with output optical fields. *Physical Review A—Atomic, Molecular, and Optical Physics*, 78(3):032316, 2008.
- [15] David Vitali, Sylvain Gigan, Anderson Ferreira, HR Böhm, Paolo Tombesi, Ariel Guerreiro, Vlatko Vedral, A Zeilinger, and Markus Aspelmeyer. Optomechanical entanglement between a movable mirror and a cavity field. *Physical review letters*, 98(3):030405, 2007.
- [16] Haixu Leng, Brian Szychowski, Marie-Christine Daniel, and Matthew Pelton. Strong coupling and induced transparency at room temperature with single quantum dots and gap plasmons. *Nature Communications*, 9(1):4012, 2018.
- [17] Xiaohua Wu, Stephen K Gray, and Matthew Pelton. Quantum-dot-induced transparency in a nanoscale plasmonic resonator. *Optics Express*, 18(23):23633–23645, 2010.
- [18] Raman A Shah, Norbert F Scherer, Matthew Pelton, and Stephen K Gray. Ultrafast reversal of a fano resonance in a plasmon-exciton system. *Physical Review B—Condensed Matter and Materials Physics*, 88(7):075411, 2013.
- [19] Mehmet Emre Tasgin, Alpan Bek, and Selen Postacı. Fano resonances in the linear and nonlinear plasmonic response. *Fano Resonances in Optics and*

- Microwaves: Physics and Applications*, 219, 2018. URL https://link.springer.com/chapter/10.1007/978-3-319-99731-5_1.
- [20] Mikhail F Limonov, Mikhail V Rybin, Alexander N Poddubny, and Yuri S Kivshar. Fano resonances in photonics. *Nature Photonics*, 11(9):543–554, 2017.
- [21] Sideband cooling is not demonstrated for plasmomechanics yet to our knowledge.
- [22] Wenchao Ge, Mehmet Emre Tasgin, and M Suhail Zubairy. Conservation relation of nonclassicality and entanglement for gaussian states in a beam splitter. *Physical Review A*, 92(5):052328, 2015.
- [23] Uwe von Lüpkke, Ines C Rodrigues, Yu Yang, Matteo Fadel, and Yiwen Chu. Engineering multimode interactions in circuit quantum acoustodynamics. *Nature Physics*, 20(4):564–570, 2024.
- [24] Koichi Murata, Yuhsuke Yasutake, Koh-ichi Nittoh, Susumu Fukatsu, and Kazushi Miki. High-density g-centers, light-emitting point defects in silicon crystal. *AIP Advances*, 1(3), 2011.
- [25] Efraim Rotem, Jeffrey M Shainline, and Jimmy M Xu. Enhanced photoluminescence from nanopatterned carbon-rich silicon grown by solid-phase epitaxy. *Applied Physics Letters*, 91(5), 2007.
- [26] Midrel Wilfried Ngandeu Ngambou, Pauline Perrin, Ionut Balasa, Alexey Tiranov, Ovidiu Brinza, Fabien Bénédic, Justine Renaud, Morgan Reveillard, Jérémie Silvent, Philippe Goldner, Jocelyn Achard, and Alexandre Tallaire. Hot ion implantation to create dense NV center ensembles in diamond. *Applied Physics Letters*, 124(13):134002, 03 2024. ISSN 0003-6951. doi: 10.1063/5.0196719.
- [27] Please note that $\omega_f = \Omega_{QE}$ when all interactions are assumed to take place at a single point, i.e., as assumed in the derivation of Eq. (1). When spatial profile of the LSP is large, e.g., in case of a 20 nm width gap, retardation effects make the Fano resonance shift substantially as we observe in Fig. 3a. Larger the LSP gap size, ω_f shifts more with respect to Ω_{QE} .
- [28] Hugo Larocque, Mustafa Atabey Buyukkaya, Carlos Errando-Herranz, Camille Papon, Samuel Harper, Max Tao, Jacques Carolan, Chang-Min Lee, Christopher JK Richardson, Gerald L Leake, et al. Tunable quantum emitters on large-scale foundry silicon photonics. *Nature Communications*, 15(1):5781, 2024.
- [29] Kenji Shibata, Hongtao Yuan, Yoshihiro Iwasa, and Kazuhiko Hirakawa. Large modulation of zero-dimensional electronic states in quantum dots by electric-double-layer gating. *Nature Communications*, 4(1):2664, 2013.
- [30] David AB Miller, DS Chemla, TC Damen, AC Gossard, W Wiegmann, TH Wood, and CA Burrus. Electric field dependence of optical absorption near the band gap of quantum-well structures. *Physical Review B*, 32(2):1043, 1985.
- [31] Michael Fleischhauer, Atac Imamoglu, and Jonathan P Marangos. Electromagnetically induced transparency: Optics in coherent media. *Reviews of Modern Physics*, 77(2):633–673, 2005.
- [32] Mehmet Emre Tasgin. Metal nanoparticle plasmons operating within a quantum lifetime. *Nanoscale*, 5(18): 8616–8624, 2013.
- [33] Fano resonances also appear when a dark plasmon mode, narrower compared to a bright mode, is coupled to a bright plasmon mode. This phenomenon, usually studied in the literature, is not to be confused with the FRs that appear due to QEs. The former ones are not so useful as the resonances of the dark plasmon modes cannot actively be tuned, e.g. via applied voltage. Moreover, FRs with dark modes are much broader compared to the ones with QEs.
- [34] Mehmet Günay, You-Lin Chuang, and Mehmet Emre Tasgin. Continuously-tunable cherenkov-radiation-based detectors via plasmon index control. *Nanophotonics*, 9(6):1479–1489, 2020.
- [35] Emre Ozan Polat, Zafer Artvin, Yusuf Şaki, Alpan Bek, and Ramazan Sahin. Continuous and reversible electrical tuning of fluorescent decay rate via fano resonance. *arXiv preprint arXiv:2412.20199*, 2024.
- [36] Sylvain Fasel, Matthäus Halder, Nicolas Gisin, and Hugo Zbinden. Quantum superposition and entanglement of mesoscopic plasmons. *New Journal of Physics*, 8(1):13, 2006.
- [37] Alexander Huck, Stephan Smolka, Peter Lodahl, Anders S Sørensen, Alexandra Boltasseva, Jiri Janousek, and Ulrik L Andersen. Demonstration of quadrature-squeezed surface plasmons in a gold waveguide. *Physical Review Letters*, 102(24):246802, 2009.
- [38] Sándor Varró, Norbert Kroó, Dániel Oszetzky, Attila Nagy, and Aladár Czitrovszky. Hanbury brown–twiss type correlations with surface plasmon light. *Journal of Modern Optics*, 58(21):2049–2057, 2011.
- [39] Giuliana Di Martino, Yannick Sonnefraud, Stéphane Kéna-Cohen, Mark Tame, Sahin K Ozdemir, MS Kim, and Stefan A Maier. Quantum statistics of surface plasmon polaritons in metallic stripe waveguides. *Nano Letters*, 12(5):2504–2508, 2012.
- [40] Sylvain Fasel, Franck Robin, Esteban Moreno, Daniel Erni, Nicolas Gisin, and Hugo Zbinden. Energy-time entanglement preservation in plasmon-assisted light transmission. *Physical Review Letters*, 94(11):110501, 2005.
- [41] Mark S Tame, KR McEnery, ŞK Özdemir, Jinhyoung Lee, Stefan A Maier, and MS Kim. Quantum plasmonics. *Nature Physics*, 9(6):329–340, 2013.
- [42] Rajiah Simon, Narasimhaiengar Mukunda, and Biswadeb Dutta. Quantum-noise matrix for multimode systems: U(n) invariance, squeezing, and normal forms. *Physical Review A*, 49(3):1567, 1994.
- [43] C. L. Garrido Alzar, M. A. G. Martinez, and P. Nussenzeig. Classical analog of electromagnetically induced transparency. *American Journal of Physics*, 70(1):37–41, 01 2002. ISSN 0002-9505. doi:10.1119/1.1412644.
- [44] Shailendra K Singh, M Kurtulus Abak, and Mehmet Emre Tasgin. Enhancement of four-wave mixing via interference of multiple plasmonic conversion paths. *Physical Review B*, 93(3):035410, 2016.
- [45] Of course, either sideband cooling or working at cryogenic temperatures is necessary for such accuracies.
- [46] See Supplemental Material at URL-will-be-inserted-by-publisher.
- [47] János K Asbóth, John Calsamiglia, and Helmut Ritsch. Computable measure of nonclassicality for light. *Physical review letters*, 94(17):173602, 2005.
- [48] Martin B Plenio. Logarithmic negativity: a full entanglement monotone that is not convex. *Physical Review Letters*, 95(9):090503, 2005.
- [49] Guifré Vidal and Reinhard F Werner. Computable mea-

- sure of entanglement. *Physical Review A*, 65(3):032314, 2002.
- [50] Mehmet Emre Tasgin. Measuring nonclassicality of single-mode systems. *Journal of Physics B: Atomic, Molecular and Optical Physics*, 53(17):175501, 2020.